3. MB INTERFERENCE

This section provides DTV susceptibility test results and characterization measurements for MB interference.

3.1. Gating Parameters

MB-OFDM achieves its ultra-wide bandwidth by simultaneously modulating 122 tones spaced 4.125 MHz apart. MB signals frequency-hop between bands according to a specified time-frequency code, which defines the number of bands (b) and the number of dwells (d) the signal stays in each band. From the perspective of a victim receiver operating within a single band, MB signals have two gating processes associated with (1) hopping and (2) insertion of zero-prefix and guard-intervals in each MB symbol. Each MB symbol is comprised of a zero-prefix (ZP), data block, and guard interval (GI); the MB symbol period is the sum of its constituents, i.e., $T_{OFDM} = T_{ZP} + T_{DATA} + T_{GI}$, where $T_{ZP} = 60.6$ ns, $T_{DATA} = 242.4$ ns, and $T_{GI} = 9.5$ ns.

Table 6 provides the MB parameters and corresponding gating parameters, i.e., on-time (τ_{on}), off-time (τ_{off}), and fractional on-time (ζ), considered in this report; these parameters also apply to GN(MB) gated-noise signals. Fractional on-time is calculated exactly as $\zeta = T_{DATA} / bT_{OFDM}$. On- and off-times are calculated as $\tau_{on} = dT_{OFDM} - T_{ZP} - T_{GI}$ and $\tau_{off} = (b - 1)dT_{OFDM} + T_{ZP} + T_{GI}$, respectively. These expressions ignore $T_{ZP} + T_{GI}$ between consecutive MB symbols and therefore are approximate in the multiple-dwell, i.e., $d > 1$, cases. This is necessary for later comparisons to *BD* and *BI* metrics and is justified for this experiment because $T_{ZP} + T_{GI} = 70.1$ ns is comparable to the reciprocal bandwidth of the victim receiver, i.e., $1/B_{DTV} = 51.3$ ns. Figure 21 illustrates gating parameters for MB-03.

Table 6. MB Gating Parameters

Type	Index	MB Parameters		Gating Parameters		
		b	d	τ_{on} (μs)	τ_{off} (μs)	ζ
MB, GN(MB)	01	1	N/A	0.24	0.07	0.776
	02	3	1	0.24	0.70	0.259
	03	3	2	0.55	1.32	0.259
	04	7	1	0.24	1.95	0.111
	05	7	2	0.55	3.82	0.111
	06	7	6	1.80	11.32	0.111
	07	13	1	0.24	3.82	0.060
	08	13	2	0.55	7.57	0.060
	09	13	12	3.68	45.07	0.060

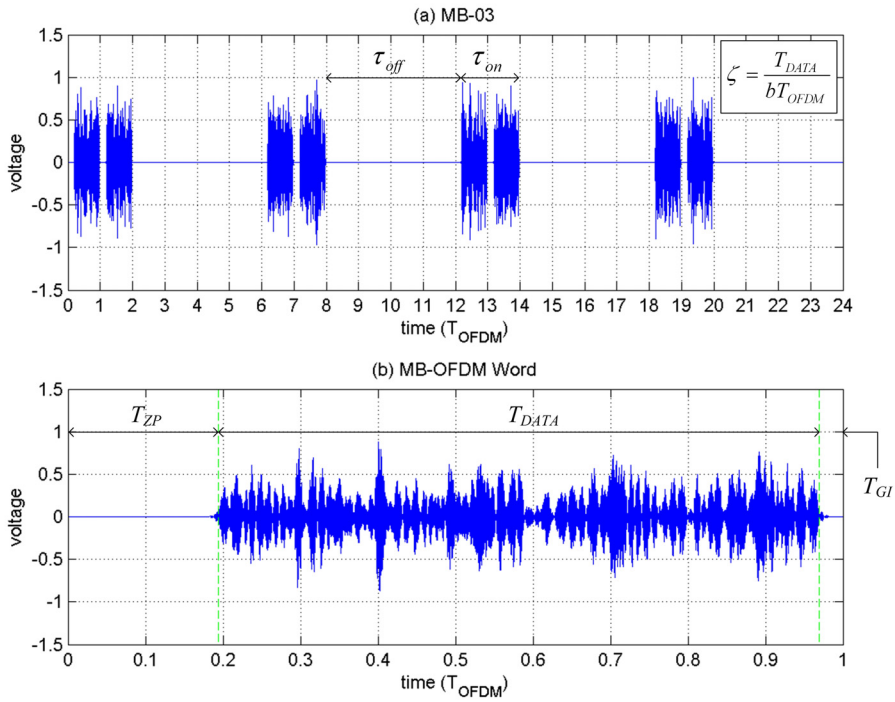

Figure 21. Simulated MB-03 transmitting random data (T_{OFDM} = 312.5 ns).

3.2. DTV Susceptibility to MB Interference

Results of the DTV susceptibility tests for MB interference are described in this section. Post-Reed-Solomon segment error rate and pre-Viterbi bit error rate are plotted versus the ratio of average interference power to average noise power. Additionally, DTV susceptibility and FEC performance metrics, i.e., INR_{TOV} and BER_{TOV}, are plotted versus $1/\zeta$ in dB.

3.2.1. DTV Signal Quality as a Function of Interference Average Power

In this subsection, *SER* and *BER* are plotted versus *INR* for DTV susceptibility to MB interference. Figures 22 – 27 provide composite plots of measured *SER* and *BER* as a function of *INR*. Each page is dedicated to a single *SNR*, each plot is dedicated to a specific range of *d*, and each curve represents a specific value of *b*. Figures 22, 24, and 26 provide composite plots of *SER*, while Figures 23, 25, and 27 provide composite plots of *BER*. For each plot, GN-01 and MB-01 results are provided as a reference.

The following are general comments regarding the shift, separation, and slope of *SER* and *BER* curves. Both *SER* and *BER* shifted toward greater *INR* with increasing *SNR*. *SER* curves with fixed *SNR* and τ_{on} show increased separation (from GN-01) with decreasing ζ. Likewise, all *SER* curves with fixed *SNR* and ζ exhibit increased separation with increasing τ_{on}. *SER* curves were generally steeper than corresponding *BER* curves. For sufficiently small ζ, slopes of the *SER* curves were not as steep as higher-ζ cases. These observations are similar to those discussed in Appendix A of Part 2 of this report series for GN(MB) gated-noise interference.

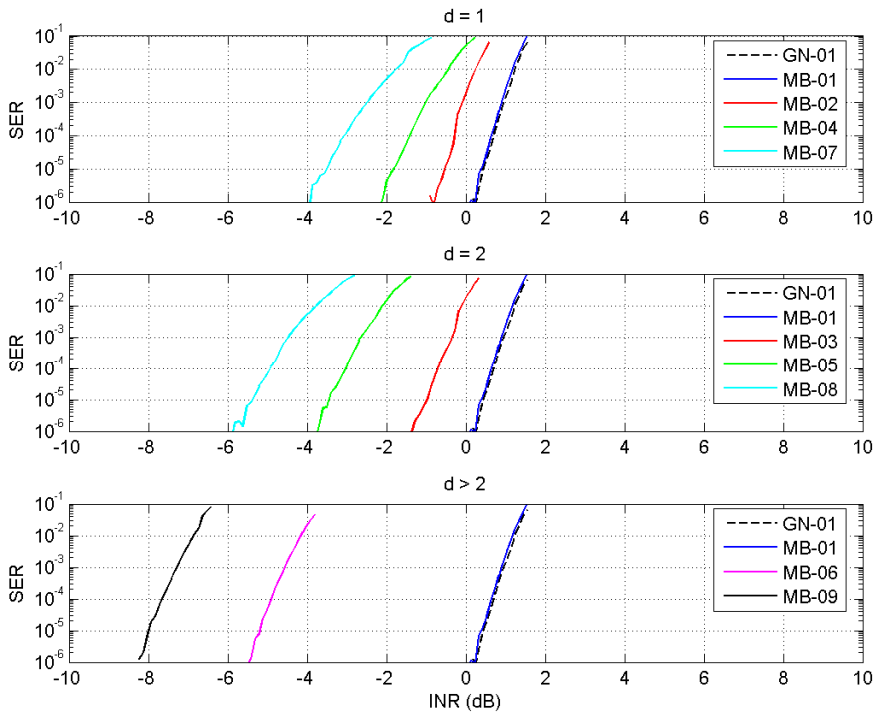

Figure 22. *SER* versus *INR* for a DTV channel operating at *SNR* = 9 dB and exposed to MB interference.

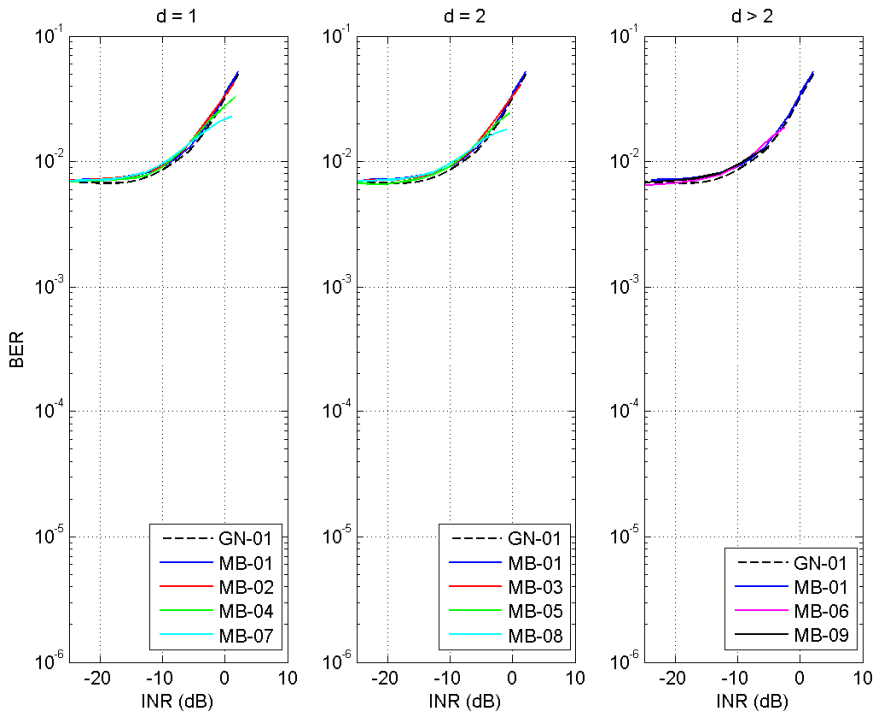

Figure 23. *BER* versus *INR* for a DTV channel operating at *SNR* = 9 dB and exposed to MB interference.

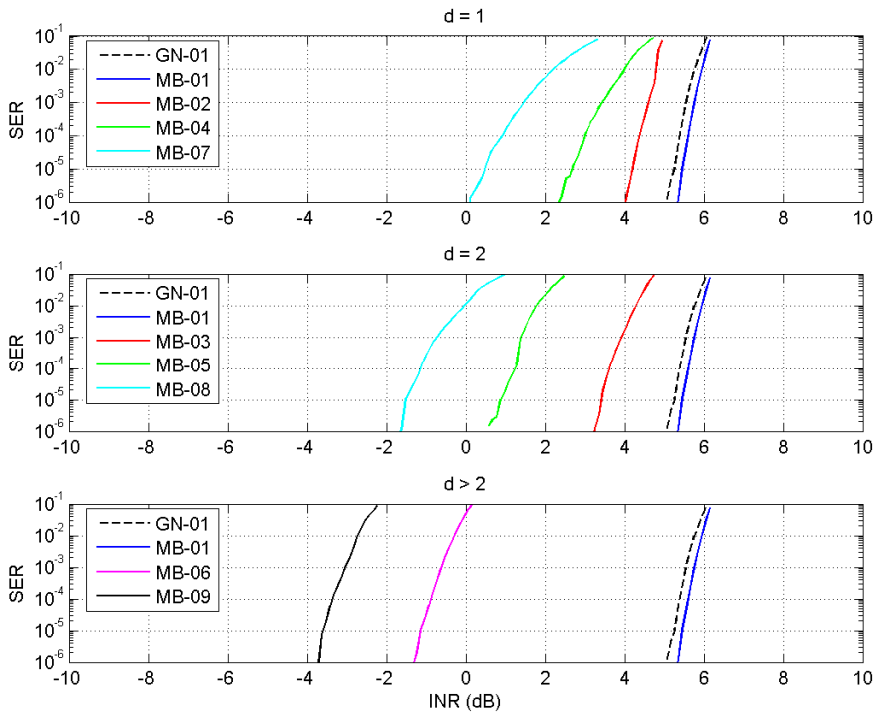

Figure 24. *SER* versus *INR* for a DTV channel operating at *SNR* = 12 dB and exposed to MB interference.

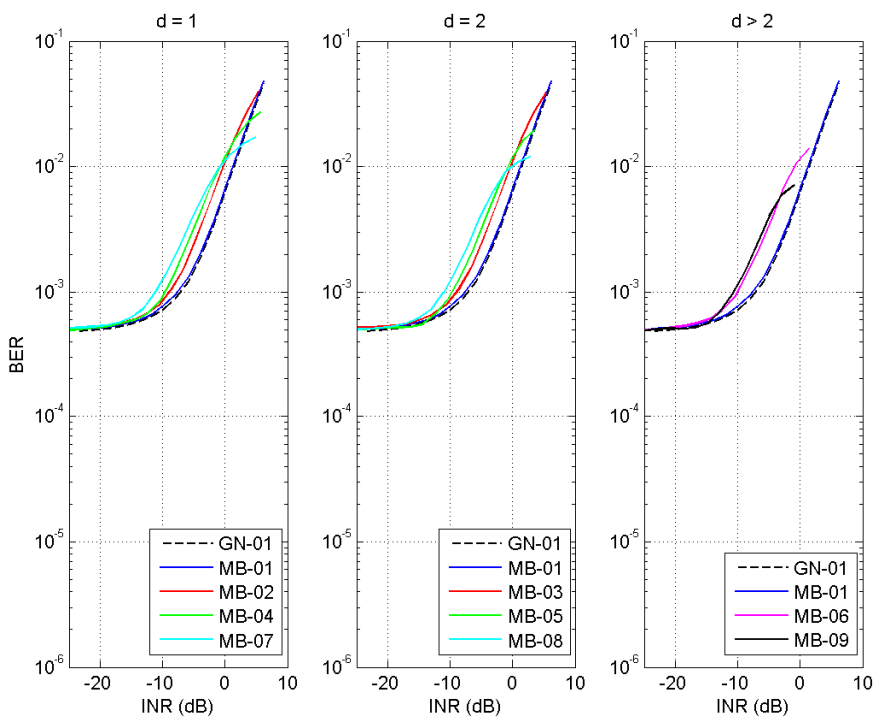

Figure 25. *BER* versus *INR* for a DTV channel operating at *SNR* = 12 dB and exposed to MB interference.

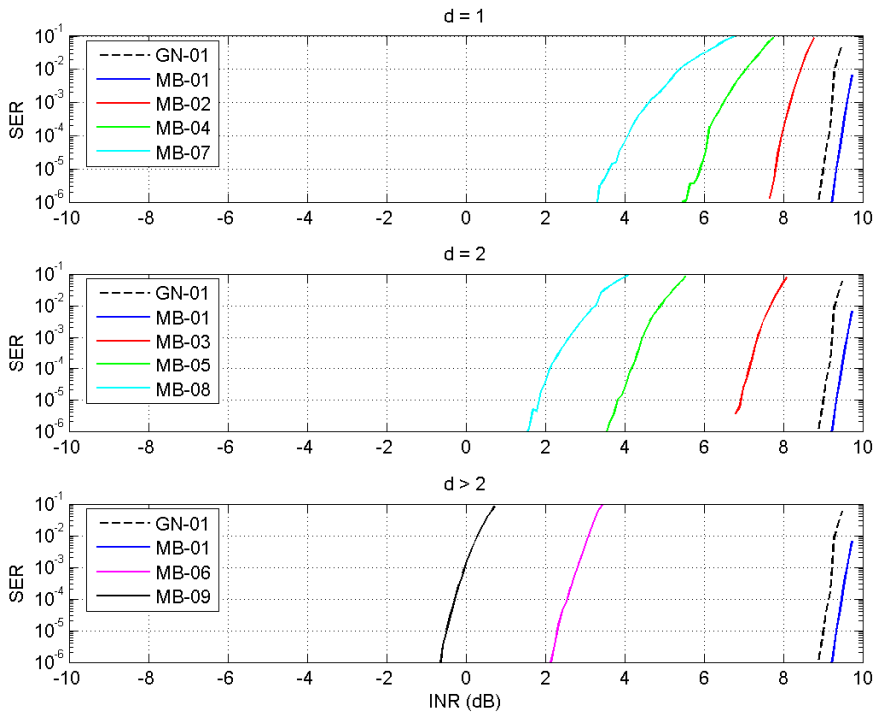

Figure 26. *SER* versus *INR* for a DTV channel operating at *SNR* = 15 dB and exposed to MB interference.

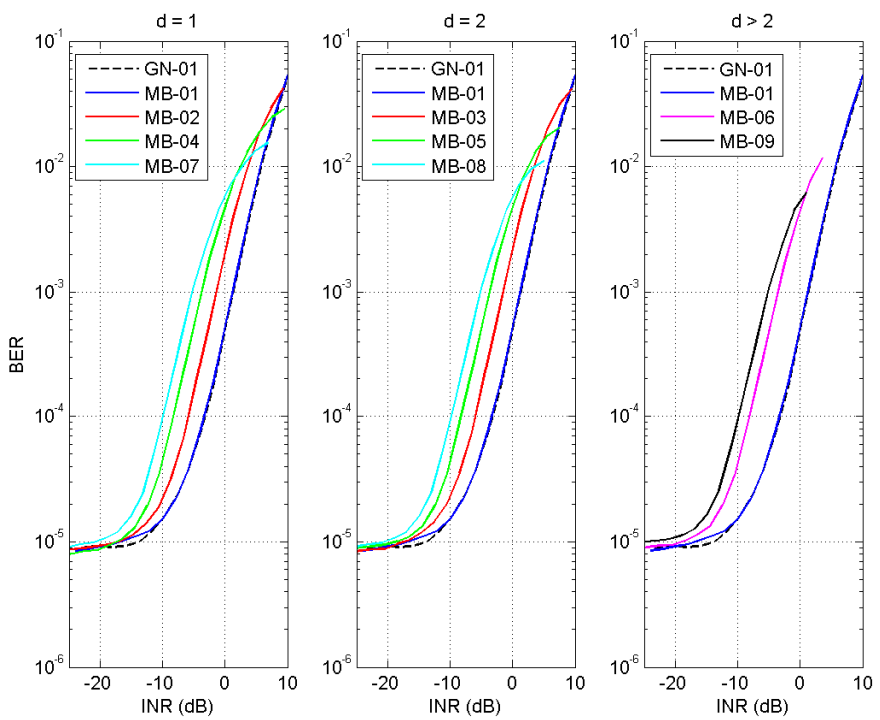

Figure 27. *BER* versus *INR* for a DTV channel operating at *SNR* = 15 dB and exposed to MB interference.

3.2.2. DTV Susceptibility as a Function of Fractional On-Time

Table 7 summarizes INR_{TOV} and BER_{TOV} results for MB interference; GN(MB) results from Part 2 of this report series are included for comparison purposes. Differences between INR_{TOV} of corresponding MB and GN(MB) results were less than 1 dB.

Table 7. Measured DTV Susceptibility and FEC Performance for MB Interference

Type	Index	*SNR* = 9 dB		*SNR* = 12 dB		*SNR* = 15 dB	
		INR_{TOV} (dB)	BER_{TOV}	INR_{TOV} (dB)	BER_{TOV}	INR_{TOV} (dB)	BER_{TOV}
MB	01	0.6	0.039	5.6	0.041	9.5	0.043
	02	-0.3	0.032	4.4	0.032	8.0	0.034
	03	-0.7	0.030	3.6	0.028	7.1	0.029
	04	-1.4	0.024	3.0	0.021	6.1	0.021
	05	-3.0	0.019	1.2	0.015	4.2	0.014
	06	-4.9	0.015	-0.9	0.010	2.6	0.010
	07	-3.1	0.018	0.9	0.013	4.1	0.021
	08	-4.9	0.015	-1.1	0.009	2.1	0.009
	09	-7.7	0.011	-3.4	0.006	-0.3	0.005
GN(MB)	01	0.5	0.037	5.2	0.036	8.5	0.036
	02	-0.7	0.030	3.7	0.027	7.0	0.028
	03	-0.9	0.028	3.5	0.025	6.5	0.025
	04	-1.9	0.022	2.3	0.018	5.8	0.019
	05	-3.2	0.018	0.8	0.013	4.2	0.013
	06	-5.0	0.015	-1.2	0.009	2.3	0.009
	07	-3.3	0.016	0.7	0.012	4.3	0.011
	08	-5.1	0.014	-1.1	0.009	2.3	0.008
	09	-7.4	0.011	-3.3	0.005	-0.3	0.005
GN	01	0.7	0.038	5.4	0.038	9.2	0.038

Figures 28 – 33 plot INR_{TOV} and BER_{TOV} versus $1/\zeta$ in dB, where $b = \{1, 3, 7, 13\}$ correspond to $\zeta = \{0.776, 0.259, 0.111, 0.060\}$ and $10\log(1/\zeta) = \{1.10, 5.87, 9.55, 12.2\}$ dB. The horizontal dashed reference line in each INR_{TOV} plot corresponds to DTV susceptibility to Gaussian noise interference. In terms of average interference power, the DTV receiver was generally more susceptible to MB signals than Gaussian noise. This is observed in Figures 28, 30, and 32 where INR_{TOV} was lower for MB-02 – MB-09 than for GN-01. Additionally, the MB results demonstrated that DTV susceptibility was dependent on temporal parameters of the interfering signal. For MB-01, τ_{off} was comparable to $1/B_{DTV}$ = 51.3 ns, and DTV susceptibility was similar to that of Gaussian noise and independent of τ_{on} and ζ. For MB-02 – MB-09, however, τ_{off} was significantly greater than $1/B_{DTV}$, and DTV susceptibility was clearly dependent on τ_{on} and ζ. More specifically, for fixed *SNR* and τ_{on}, DTV susceptibility increased with decreasing ζ. Likewise, for fixed *SNR* and ζ, DTV susceptibility increased with increasing τ_{on}.

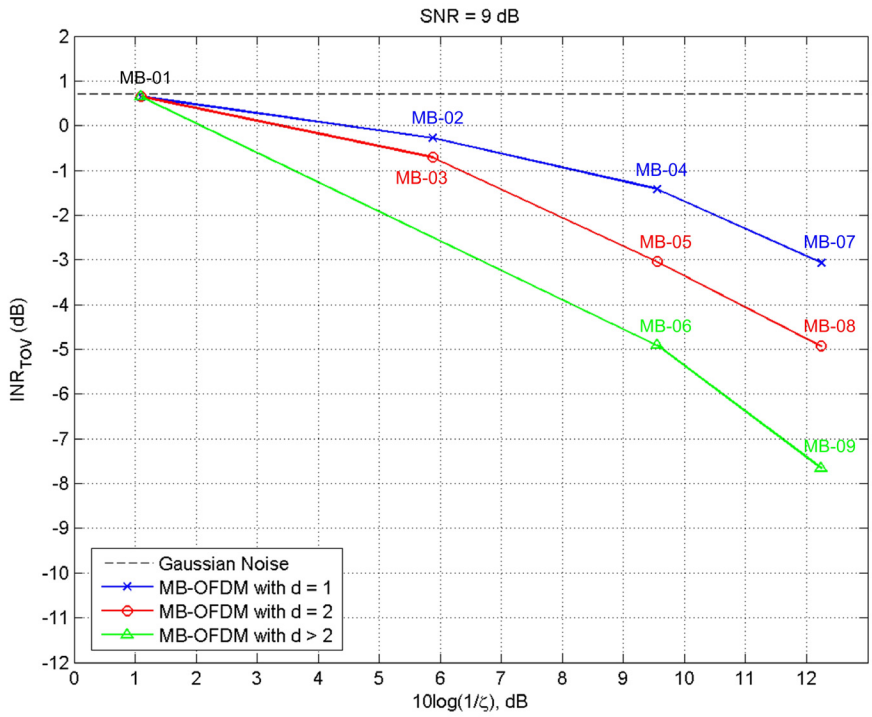

Figure 28. INR_{TOV} versus 10log(1/ζ) for a DTV channel operating at SNR = 9 dB and exposed to MB interference.

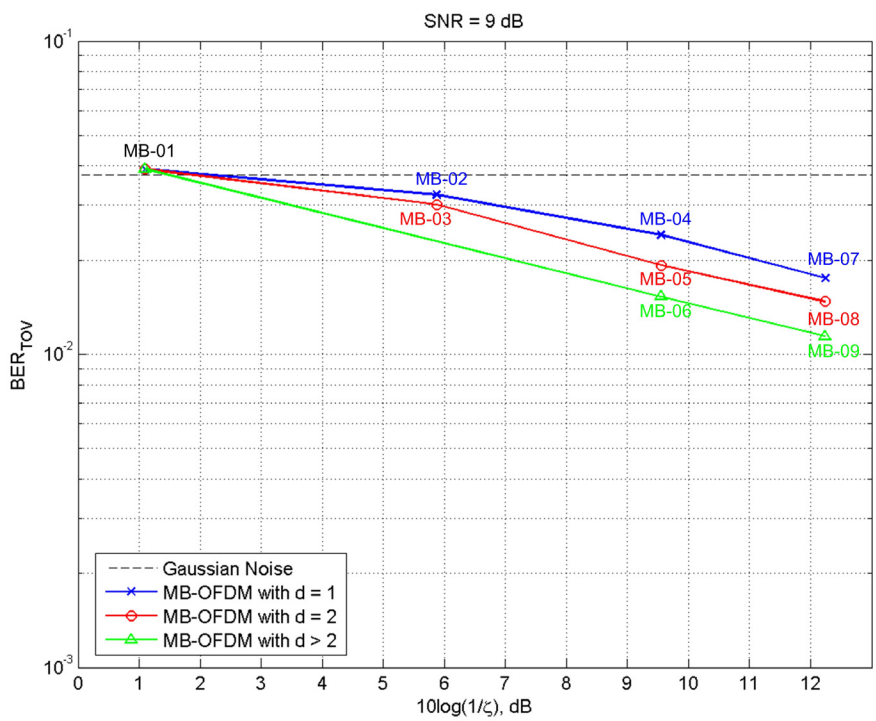

Figure 29. BER_{TOV} versus 10log(1/ζ) for a DTV channel operating at SNR = 9 dB and exposed to MB interference.

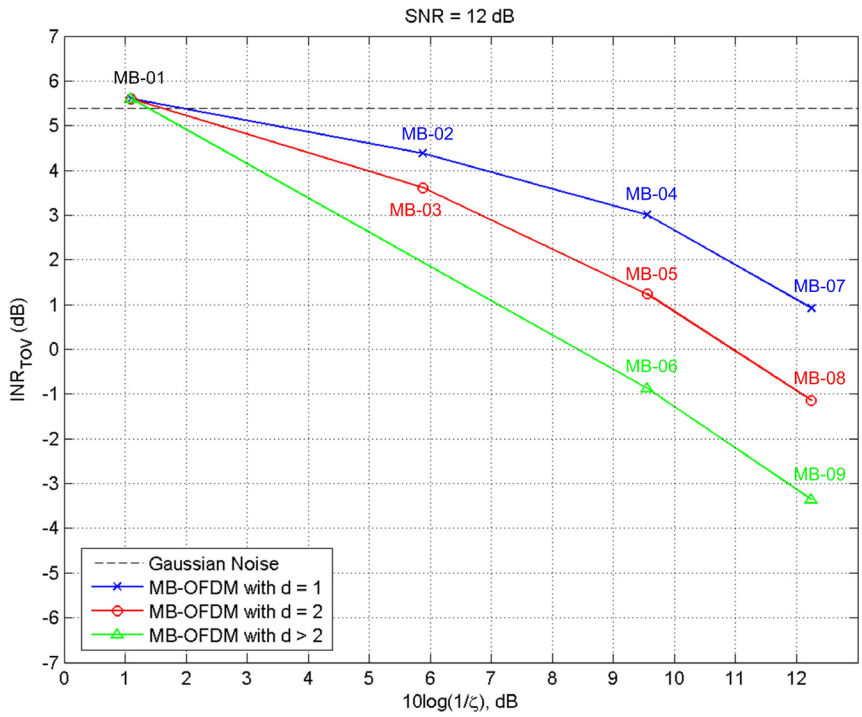

Figure 30. INR_{TOV} versus 10log(1/ζ) for a DTV channel operating at SNR = 12 dB and exposed to MB interference.

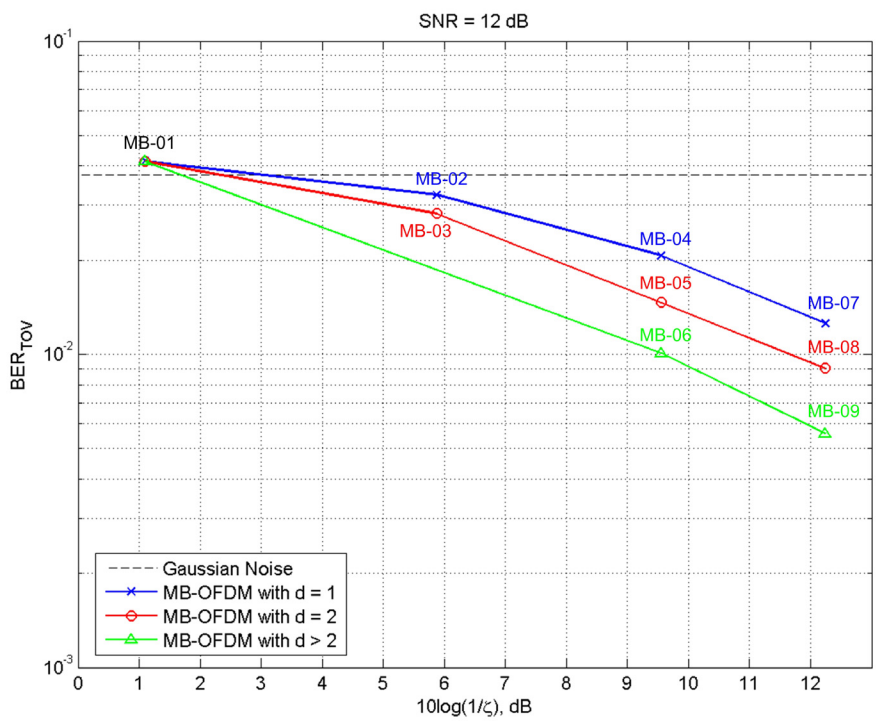

Figure 31. BER_{TOV} versus 10log(1/ζ) for a DTV channel operating at SNR = 12 dB and exposed to MB interference.

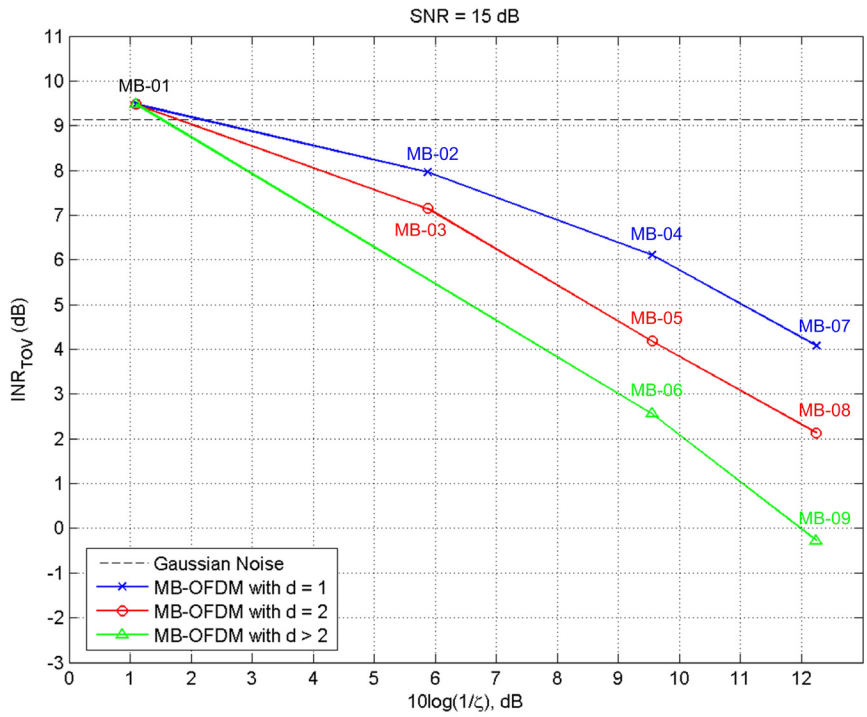

Figure 32. INR_{TOV} versus 10log(1/ζ) for a DTV channel operating at SNR = 15 dB and exposed to MB interference.

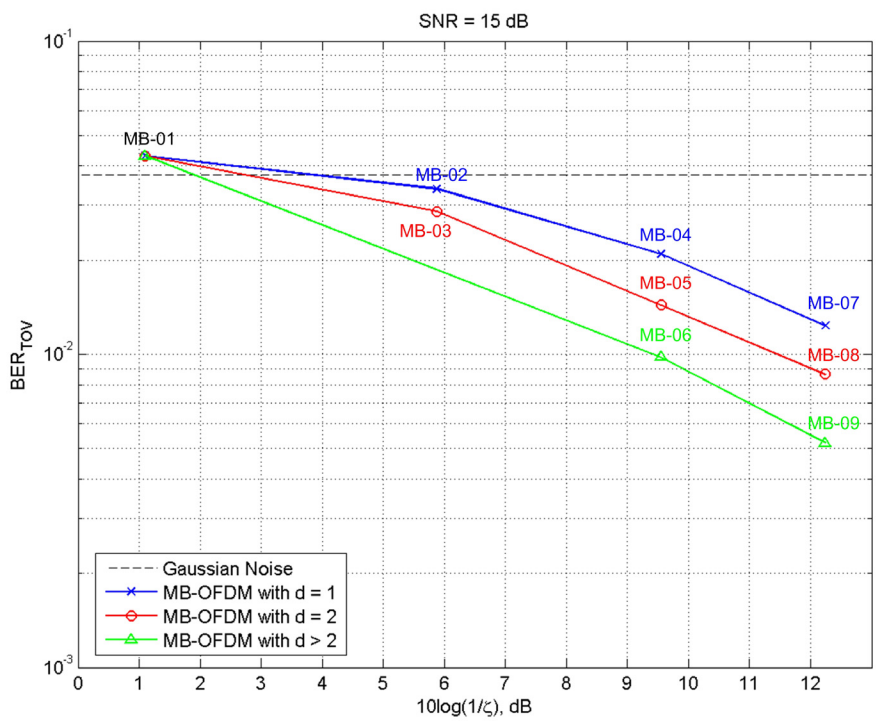

Figure 33. BER_{TOV} versus 10log(1/ζ) for a DTV channel operating at SNR = 15 dB and exposed to MB interference.

3.3. Characterization of MB Signals

Characterization of MB signals was accomplished via temporal, amplitude, and spectral analyses. This section provides band-limited signal characterization results for the B_{DTV} = 19.51-MHz DTV receiver RRC filter.

3.3.1. Temporal Analysis

Table 8 summarizes the effects of band-limiting on the temporal characteristics of MB signals. As expected, band-limiting lengthened on-times, $BD > \tau_{on}$, shortened off-times, $BI < \tau_{off}$, and increased fractional on-times, $\zeta_{DTV} > \zeta$. *BD* and *BI* approached the respective gating parameters only when τ_{on} and τ_{off} were significantly larger than $1/B_{DTV}$. Notice that measured MB temporal characteristics are identical to those of the GN(MB) signals.

Table 8. Measured Temporal Characteristics of MB Signals Band-Limited to B_{DTV}

Index	Gating Parameters			MB			GN(MB)		
	τ_{on} (μs)	τ_{off} (μs)	ζ	*BD* (μs)	*BI* (μs)	ζ_{DTV}	*BD* (μs)	*BI* (μs)	ζ_{DTV}
01	0.24	0.07	0.776	3.7	0.0	1.00	3.7	0.0	1.00
02	0.24	0.70	0.259	0.4	0.6	0.40	0.4	0.6	0.40
03	0.55	1.32	0.259	0.7	1.2	0.37	0.7	1.2	0.37
04	0.24	1.95	0.111	0.4	1.8	0.18	0.4	1.8	0.18
05	0.55	3.82	0.111	0.7	3.7	0.16	0.7	3.7	0.16
06	1.80	11.32	0.111	1.9	11.2	0.15	1.9	11.2	0.15
07	0.24	3.82	0.060	0.4	3.7	0.10	0.4	3.7	0.10
08	0.55	7.57	0.060	0.7	7.4	0.09	0.7	7.4	0.09
09	3.68	45.07	0.060	2.5	44.9	0.05	2.5	44.9	0.05

3.3.2. Amplitude Analysis

Figures 34 and 35 provide composite *APD* plots of measured single- and multi-dwell MB signals, respectively. Notice that measured average powers, indicated in the legends, were proportional to ζ. Band-limiting had profound effects on the *APD*s of the MB signals. For MB-01, τ_{off} was less than or comparable to $1/B_{DTV}$ and a negatively-sloped, relatively straight *APD* occurred. For MB-02 – MB-09, τ_{off} exceeded $1/B_{DTV}$ and a step-like *APD* occurred where higher amplitudes corresponded to MB interference during elongated on-times and lower amplitudes corresponded to system noise observable during shortened off-times. This was most pronounced for MB-08 and MB-09.

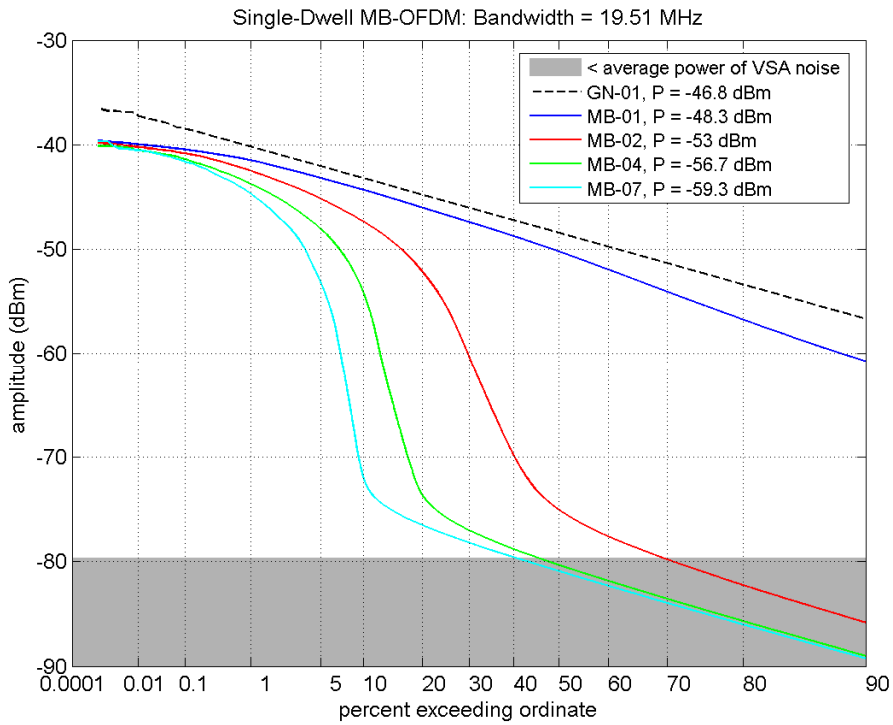

Figure 34. *APD*s of single-dwell MB signals band-limited to B_{DTV}.

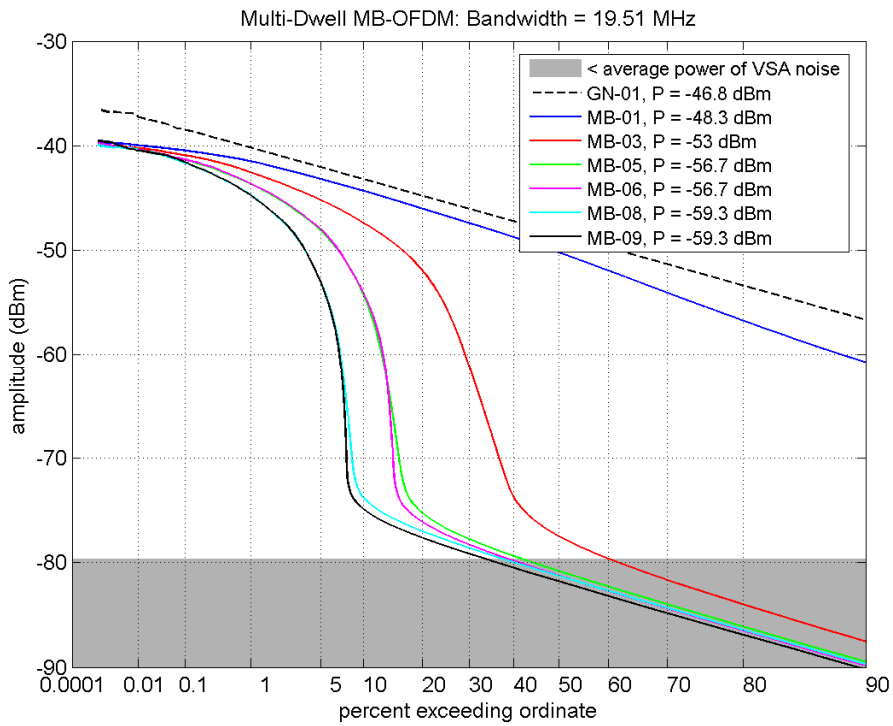

Figure 35. *APD*s of multi-dwell MB signals band-limited to B_{DTV}.

Table 9 summarizes measured *P/A* and *APD* characteristics for the MB signals band-limited to B_{DTV}. *APD* characteristics are labeled RG for resolved gating, i.e., step-like *APD* whose amplitude falls below the average power of the VSA noise at least 10% of the time. Notice that measured *P/A*s of the MB signals were 1 – 2 dB less than the *P/A* of corresponding GN(MB) signals.

Table 9. Measured Amplitude Characteristics of MB Signals Band-Limited to B_{DTV}

Index	MB		GN(MB)	
	P/A (dB)	*APD*	*P/A* (dB)	*APD*
01	8.3		10.5	
02	12.8	RG	14.7	RG
03	12.8	RG	14.6	RG
04	16.2	RG	18.0	RG
05	16.4	RG	17.9	RG
06	16.3	RG	17.8	RG
07	18.7	RG	20.2	RG
08	18.9	RG	20.1	RG
09	18.8	RG	19.9	RG

3.3.3. Spectral Analysis

Figures 36 and 37 provide measured *PSD*s of the single- and multi-dwell MB signals, respectively, over the VSA bandwidth. In Figure 37, the *PSD* of MB-05 is directly beneath MB-06. To compute the *PSD*, 500 blocks of length = 170.6 µs (Δf = 5.9 kHz) were averaged. Measured MB *PSD*s were flat across the band of interest, and measured power density was proportional to ζ. Differences between measured MB and GN(MB) *PSD*s were negligible. Also, the spectral line at 0 Hz was due to VSG local-oscillator feed-through. The influence of the VSG local-oscillator feed-through on test results was discussed in Appendix C of Part 1 of this report series.

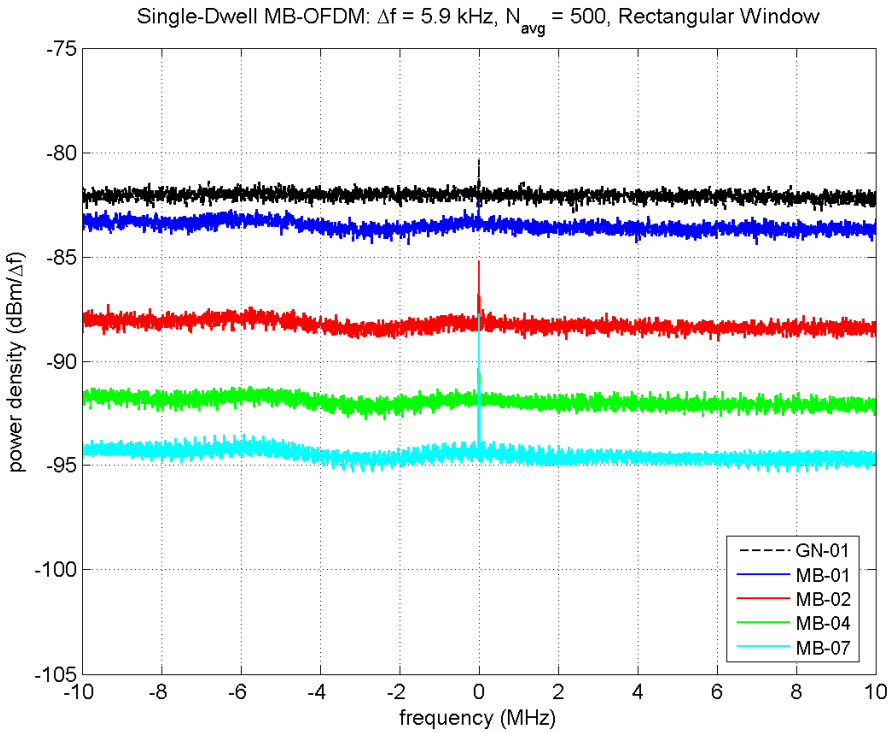

Figure 36. *PSD*s of single-dwell MB signals.

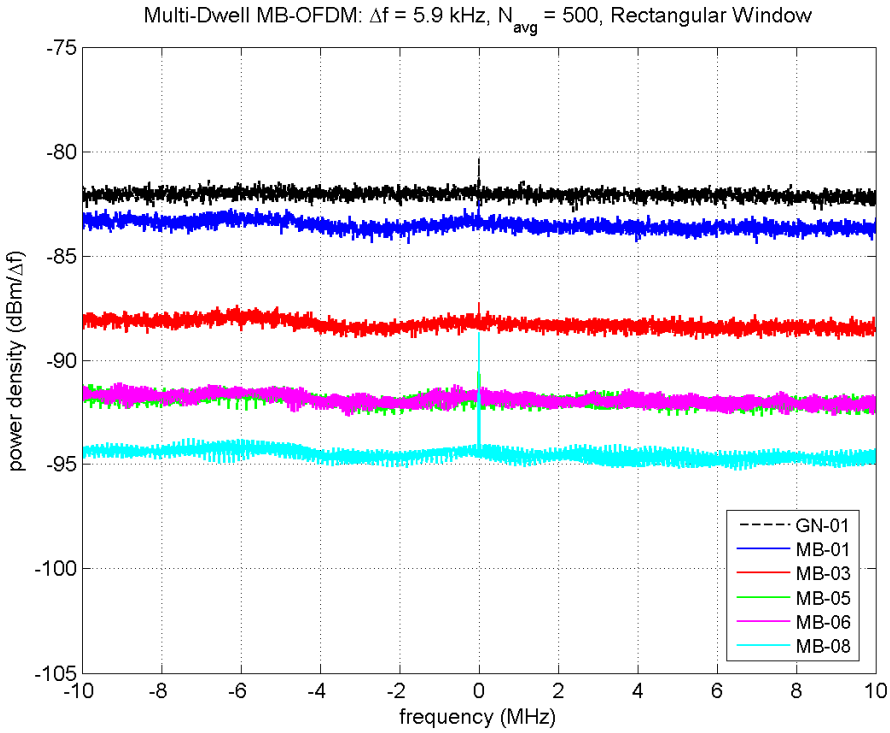

Figure 37. *PSD*s of multi-dwell MB signals.